

# Chapter 10

## The One-Dimensional Stationary SCHRÖDINGER Equation

### 10.1 Introduction

The numerical solution of the stationary SCHRÖDINGER equation is discussed to illustrate the application of NUMEROV's shooting method introduced in Sect. 8.3.

We start the discussion with a brief survey of basic quantum mechanics. Of course, this chapter is not supposed to give a self-contained introduction into this field and the reader not familiar with quantum mechanics should, therefore, regard the following discussion from a purely mathematical point of view. For more in-depth reading on quantum mechanics we refer to the books [1–4] to name a few.

A quantum-mechanical wave-function  $\Psi \equiv \Psi(x, t) \in \mathbb{C}$  is a function of time  $t \in \mathbb{R}^+$  and space  $x \in \mathbb{R}^3$  and obeys the SCHRÖDINGER equation:

$$i\hbar \frac{d}{dt} \Psi = H\Psi . \tag{10.1}$$

Here,  $\hbar = h/(2\pi)$  is the reduced PLANCK constant,  $i$  is the imaginary unit, and  $H$  is the HAMILTON operator or Hamiltonian. If  $H \neq H(t)$ , i.e. the Hamiltonian is independent of time  $t$ , we can employ a product ansatz

$$\Psi(x, t) = \exp\left(-\frac{i}{\hbar}Et\right) \psi(x) , \tag{10.2}$$

where  $E$  is the energy and  $\psi(x)$  is the time-independent part of the wave-function. This ansatz transforms Eq. (10.1) into

$$\begin{aligned} i\hbar \frac{d}{dt} \left[ \exp\left(-\frac{i}{\hbar}Et\right) \psi(x) \right] &= i\hbar \left(-\frac{i}{\hbar}E\right) \exp\left(-\frac{i}{\hbar}Et\right) \psi(x) \\ &= \exp\left(-\frac{i}{\hbar}Et\right) H\psi(x), \end{aligned} \quad (10.3)$$

and  $\psi(x)$  is determined by the eigenvalue problem [5]

$$H\psi = E\psi, \quad (10.4)$$

augmented by appropriate boundary conditions. We already came across Eq. (10.4) when we discussed shooting methods in Sect. 8.3.

The one-particle Hamiltonian is of the general form

$$H = T + V = \frac{P^2}{2m} + V, \quad (10.5)$$

with the kinetic energy operator  $T$ , the potential operator  $V$ , the momentum operator  $P$ , and the particle's mass  $m$ . If the system is not exposed to an external magnetic field,  $P$  can be expressed in position space by

$$P = -i\hbar\nabla, \quad (10.6)$$

and the potential operator  $V$  by  $V(x)$ . Thus we get for Eq. (10.5):

$$H = -\frac{\hbar^2}{2m}\Delta + V(x). \quad (10.7)$$

Hence, we have to solve the linear, second order partial differential equation:

$$-\frac{\hbar^2}{2m}\Delta\psi(x) + V(x)\psi(x) = E\psi(x). \quad (10.8)$$

This equation will certainly not have solutions for arbitrary values of the energy  $E$ . The particular values  $E = E_n$ <sup>1</sup> for which it has a solution are referred to as *eigenenergies* and the corresponding solution  $\psi_n(x)$  is referred to as *eigenfunction*

---

<sup>1</sup>It depends on the problem on hand whether or not the index  $n$  will be continuous or discrete. For simplicity, we assume here  $n$  to be discrete.

to the eigenenergy  $E_n$  [1–3, 5]. To emphasize this point we rewrite Eq. (10.8) as:

$$-\frac{\hbar^2}{2m}\Delta\psi_n(x) + V(x)\psi_n(x) = E_n\psi_n(x), \quad \forall n \in \mathbb{N}. \quad (10.9)$$

It is the purpose of this chapter to develop a numerical procedure which will, in the end, allow to calculate numerically the eigenvalues  $E_n$  and eigenfunctions  $\psi_n(x)$  as solutions of this equation.

We proceed in our analysis by defining the scalar product between two functions  $\chi(x)$  and  $\varphi(x)$

$$\langle \chi | \varphi \rangle = \int dx \chi^*(x)\varphi(x), \quad (10.10)$$

where  $\chi^*(x)$  denotes the complex conjugate of  $\chi(x)$ . The corresponding  $L^2$ -norm reads

$$|\chi| = \sqrt{\langle \chi | \chi \rangle} = \sqrt{\int dx |\chi(x)|^2}. \quad (10.11)$$

The expectation value of an operator  $O$  in the quantum mechanical state  $\Psi$  is given by

$$\langle O \rangle = \frac{\langle \Psi | O | \Psi \rangle}{\langle \Psi | \Psi \rangle} = \frac{\int dx \Psi^*(x) O \Psi(x)}{\int dx |\Psi(x)|^2}. \quad (10.12)$$

It follows from Eq. (10.4) that the energy is the expectation value of the Hamiltonian  $H$

$$\langle H \rangle = \frac{\int dx \Psi^*(x) H \Psi(x)}{\int dx |\Psi(x)|^2} = E. \quad (10.13)$$

We quote now some important properties; a detailed discussion can be found in any textbook on quantum mechanics.

- The expectation value  $\langle O \rangle$  of a Hermitian operator  $O$ ,  $O^\dagger = O$ , is real, i.e.  $\langle O \rangle = \langle O \rangle^*$ . Here  $O^\dagger$  denotes the adjoint of  $O$ , i.e.  $O^\dagger = (O^*)^T$ .
- Every real expectation value can be described by a Hermitian operator.
- All observables can be described by Hermitian operators, in particular, the Hamiltonian *has* to be a *Hermitian* operator to ensure that the eigenenergies  $E_n$  are real,  $E_n \in \mathbb{R}$ .

- It follows from the hermiticity of  $H$  that the eigenfunctions  $\psi_n(x)$  form a complete, orthogonal basis in HILBERT space [5]. Furthermore, the functions can be normalized and the relation

$$\langle \psi_n | \psi_m \rangle = \delta_{nm} , \quad (10.14)$$

holds, with  $\delta_{nm}$  the KRONECKER- $\delta$ .

Thus, with the help of Eq. (10.14) we rewrite the expectation value (10.12) of a Hermitian operator  $O$  as:

$$\langle O \rangle = \int dx \Psi^*(x) O \Psi(x) . \quad (10.15)$$

In a next step we define the wave function  $\Psi_n(x, t)$  following the ansatz (10.2)

$$\Psi_n(x, t) = \exp\left(-\frac{i}{\hbar} E_n t\right) \psi_n(x) , \quad (10.16)$$

and the total wave-function  $\Psi(x, t)$  is then a superposition of wave-functions  $\Psi_n(x, t)$

$$\Psi(x, t) = \sum_n c_n \Psi_n(x, t) , \quad (10.17)$$

because the  $\Psi_n(x, t)$  constitute a complete, orthogonal basis.<sup>2</sup> Furthermore, we demand  $\Psi(x, t)$  to be normalized for all  $t$ . Employing Eq. (10.14) in Eq. (10.17) yields

$$\int dx |\Psi(x, t)|^2 = \sum_n |c_n|^2 = 1 . \quad (10.18)$$

We quote BORN's interpretation of the squared modulus of the total wave-function (referred to as BORN's rule):

$$\begin{aligned} |\Psi(x, t)|^2 dx = & \text{The probability that the particle described by} \\ & \text{the wave-function } \Psi(x, t) \text{ can be found at time} \\ & t \text{ within a volume } dx \text{ around the point } x. \end{aligned} \quad (10.19)$$

---

<sup>2</sup>This is only possible because the SCHRÖDINGER equation is linear.

This interpretation justifies the requirement of a normalization of the wave-function  $\Psi(x, t)$

$$\int dx |\Psi(x, t)|^2 \stackrel{!}{=} 1, \quad (10.20)$$

because, by definition, the particle has to be found somewhere anytime.

Suppose we start with an initial state  $\chi(x) = \Psi(x, t = 0)$ . Since the functions  $\psi_n(x)$  form a complete basis in HILBERT space,  $\chi(x)$  may be written with the help of Eq. (10.17) as

$$\chi(x) = \sum_n c_n \psi_n(x). \quad (10.21)$$

We deduce from Eq. (10.14) that

$$\langle \psi_m | \chi \rangle = \sum_n c_n \int dx \psi_m^*(x) \psi_n(x) = c_m. \quad (10.22)$$

Consequently,  $|c_m|^2$  is the probability that the particle was initially in state  $m$ . This allows us to interpret Eq. (10.17) in the following way: The coefficients  $c_m$  determine the composition of the initial state. The exponential factor describes an oscillation and we note that different eigenfunctions, which correspond to different eigenenergies, oscillate with different frequencies. This can, for instance, induce the diffidence of a wave packet.

## 10.2 A Simple Example: The Particle in a Box

We concentrate on the one-dimensional SCHRÖDINGER equation and discuss a simple problem which will then be solved numerically in Sect. 10.3. We rewrite the one-dimensional SCHRÖDINGER equation (10.7), with  $x \in \mathbb{R}$ , as

$$-\frac{\hbar^2}{2m} \frac{d^2}{dx^2} \psi_n(x) + V(x) \psi_n(x) = E_n \psi_n(x), \quad (10.23)$$

and specify

$$V(x) = \begin{cases} 0 & 0 \leq x \leq L, \\ \infty & \text{elsewhere,} \end{cases} \quad (10.24)$$

together with the boundary conditions

$$\psi_n(0) = \psi_n(L) = 0, \quad (10.25)$$

and the normalization condition

$$\int_0^L dx |\psi_n(x)|^2 = \int_0^L dx |\psi_n(x)|^2 = 1. \quad (10.26)$$

We note that the boundary conditions are dictated by the particular form of the potential (10.24) which requires that  $\psi_n(x) = 0$  for  $x \notin [0, L]$ . This problem is commonly referred to as the *particle in a one-dimensional box*.

Let us introduce dimensionless variables in order to simplify the numerics of Eq. (10.23). We define new variables

$$s = \frac{x}{L}, \quad \varepsilon_n = \frac{E_n}{\bar{E}}, \quad (10.27)$$

where  $L$  is the length scale and  $\bar{E}$  is the energy scale. The energy scale  $\bar{E}$  is fully determined by the relation

$$\bar{E} = \frac{\hbar^2}{mL^2}. \quad (10.28)$$

We note that  $s \in [0, 1]$ , hence the rescaled wave-function is given by

$$\varphi_n(s) = \sqrt{L} \psi_n(x), \quad (10.29)$$

which satisfies the normalization condition

$$\int_0^L dx |\psi_n(x)|^2 = \int_0^1 ds |\varphi_n(s)|^2 = 1. \quad (10.30)$$

The rescaled SCHRÖDINGER equation can be obtained by multiplying Eq. (10.23) with  $1/\bar{E}$ :

$$\begin{aligned} -\frac{\hbar^2}{2m\bar{E}} \frac{d^2}{dx^2} \psi_n(x) + \frac{V(x)}{\bar{E}} \psi_n(x) &= -\frac{L^2}{2} \frac{d^2}{dx^2} \psi_n(x) + v(s) \psi_n(x) \\ &= -\frac{1}{2} \frac{d^2}{ds^2} \psi_n(x) + v(s) \psi_n(x) \\ &= \frac{E_n}{\bar{E}} \psi_n(x) \\ &= \varepsilon_n \psi_n(x). \end{aligned} \quad (10.31)$$

Here we introduced the rescaled potential  $v(s)$

$$v(s) = \begin{cases} 0 & 0 \leq s \leq 1, \\ \infty & \text{elsewhere.} \end{cases} \quad (10.32)$$

Hence, the rescaled wave-function (10.29) is a solution of the differential equation:

$$-\frac{1}{2} \frac{d^2}{ds^2} \varphi_n(s) + v(s)\varphi_n(s) = \varepsilon_n \varphi_n(s). \quad (10.33)$$

The form (10.32) of the potential implies that  $\varphi_n(s) = 0$  for all  $s \notin [0, 1]$  and the complete boundary value problem is defined as:

$$\begin{cases} -\frac{1}{2} \frac{d^2}{ds^2} \varphi_n(s) = \varepsilon_n \varphi_n(s), & s \in [0, 1], \\ \varphi_n(0) = 0, \\ \varphi_n(1) = 0. \end{cases} \quad (10.34)$$

It is an easy task to solve this boundary value problem analytically. For  $s \in [0, 1]$  we choose the ansatz

$$\varphi_n(s) = A_n \sin(k_n s) + B_n \cos(k_n s), \quad (10.35)$$

where  $A_n$  and  $B_n$  are some constants and  $k_n$  is given by

$$k_n = \sqrt{2\varepsilon_n}. \quad (10.36)$$

From the boundary conditions we obtain

$$\varphi_n(0) = B_n = 0, \quad (10.37)$$

and

$$\varphi_n(1) = A_n \sin(k_n) = 0. \quad (10.38)$$

Thus,

$$k_n = n\pi , \quad (10.39)$$

and the eigenenergies  $\varepsilon_n$  are quantized:

$$\varepsilon_n = \frac{n^2 \pi^2}{2} . \quad (10.40)$$

The corresponding eigenfunctions  $\varphi_n(s)$  are then given by:

$$\varphi_n(s) = \begin{cases} A_n \sin(n\pi s) & s \in [0, 1] , \\ 0 & \text{elsewhere.} \end{cases} \quad (10.41)$$

The constants  $A_n$  are determined from the normalization condition (10.30)<sup>3</sup>

$$\begin{aligned} \int_0^1 ds |\varphi_n(s)|^2 &= A_n^2 \int_0^1 ds \sin^2(n\pi s) \\ &= \frac{A_n^2}{2} \\ &\stackrel{!}{=} 1 , \end{aligned} \quad (10.43)$$

and:

$$A_n = \sqrt{2} . \quad (10.44)$$

Finally, we apply the relations (10.27), (10.28), and (10.29) and obtain

$$\psi_n(x) = \frac{1}{\sqrt{L}} \varphi_n\left(\frac{x}{L}\right) = \begin{cases} \sqrt{\frac{2}{L}} \sin\left(\frac{n\pi x}{L}\right) & x \in [0, L] , \\ 0 & \text{elsewhere,} \end{cases} \quad (10.45)$$

---

<sup>3</sup> Here we make use of

$$\int du \sin^2(u) = \frac{1}{2} [u - \cos(u) \sin(u)] . \quad (10.42)$$

and

$$E_n = \varepsilon_n \bar{E} = \frac{\hbar^2 \pi^2 n^2}{2mL^2} . \quad (10.46)$$

In most cases expectation values of some observables are to be determined. We might, for instance, be interested in the expectation value  $\langle x \rangle$  of the position operator  $x$  or its variance  $\text{var}(x) = \langle (x - \langle x \rangle)^2 \rangle$  (see also Appendix E). It follows from Eq. (10.27) that

$$\langle x \rangle = L \langle s \rangle , \quad \text{and} \quad \langle (x - \langle x \rangle)^2 \rangle = L^2 \langle (s - \langle s \rangle)^2 \rangle = L^2 \text{var}(s) . \quad (10.47)$$

Definition (10.15) gives together with solution (10.41) the expectation value  $\langle s \rangle$ :

$$\langle s \rangle = 2 \int_0^1 ds \sin^2(n\pi s) s = \frac{1}{2} . \quad (10.48)$$

Thus, the expectation value of the position operator is independent of the quantum number  $n$ . Furthermore, we obtain for  $\langle s^2 \rangle$ :

$$\langle s^2 \rangle = 2 \int_0^1 ds \sin^2(n\pi s) s^2 = \frac{1}{3} - \frac{1}{2n^2\pi^2} . \quad (10.49)$$

Hence, the variance  $\text{var}(s)$  is determined by

$$\langle (s - \langle s \rangle)^2 \rangle = \langle s^2 \rangle - \langle s \rangle^2 = \frac{1}{3} - \frac{1}{2n^2\pi^2} - \frac{1}{4} = \frac{1}{12} \left( 1 - \frac{6}{n^2\pi^2} \right) . \quad (10.50)$$

We note that the variance increases with increasing  $n$ .

In the next section these results are reproduced numerically by the NUMEROV shooting method. (See Sect. 8.3 and, for instance, Ref. [6].) Moreover, this numerical formulation will allow us to find solutions for more complex potentials  $V(x)$ .

## 10.3 Numerical Solution

The following discussion is based on the scaled SCHRÖDINGER equation (10.33), but we consider now a more general potential of the form

$$v(s) = \begin{cases} \tilde{v}(s) & 0 \leq s \leq 1 , \\ \infty & \text{elsewhere,} \end{cases} \quad (10.51)$$

which results in the boundary value problem:

$$\left\{ \begin{array}{l} -\frac{1}{2} \frac{d^2}{ds^2} \varphi_n(s) + \tilde{v}(s) \varphi_n(s) = \varepsilon_n \varphi_n(s) \quad s \in [0, 1], \quad n \in \mathbb{N}, \\ \varphi_n(0) = 0, \\ \varphi_n(1) = 0. \end{array} \right. \quad (10.52)$$

As our numerical treatment will be based on shooting methods, discussed in Sect. 8.3, the second order differential equation in Eq. (10.52) will be transformed into a form which corresponds to Eq. (8.54), namely:

$$\varphi_n''(s) + 2[\varepsilon_n - \tilde{v}(s)] \varphi_n(s) = 0. \quad (10.53)$$

The interval  $[0, 1]$  is discretized using  $N + 1$  grid-points  $s_\ell = \ell/N$ ,  $\ell = 0, 1, 2, \dots, N$  ( $h = 1/N$ ) and we denote with  $\varphi_n(s_\ell)$  and  $\tilde{v}(s_\ell) \equiv v_\ell$  the values of  $\varphi_n(s)$  and  $\tilde{v}(s)$  at those grid-points. Thus, Eq. (8.59) can immediately be applied and we get:

$$\varphi_n(s_{\ell+1}) = \frac{2 \left[ 1 - \frac{5}{6N^2} (\varepsilon_n - \tilde{v}_\ell) \right] \varphi_n(s_\ell) - \left[ 1 + \frac{1}{6N^2} (\varepsilon_n - \tilde{v}_{\ell-1}) \right] \varphi_n(s_{\ell-1})}{1 + \frac{1}{6N^2} (\varepsilon_n - \tilde{v}_{\ell+1})}. \quad (10.54)$$

We use the initial conditions  $\varphi_n(s_0) = 0$  and  $\varphi_n'(s_0) = 1$ , which is always possible, since (10.52) is a homogeneous boundary value problem. This gives

$$\varphi_n'(s_0) \approx \frac{\varphi_n(s_1) - \varphi_n(s_{-1})}{2h} = 1 \quad \Rightarrow \quad \varphi_n(s_1) = \frac{2}{N}. \quad (10.55)$$

The normalization of the wave-function (10.30) is then approximated with the help of the forward rectangular rule (3.9):

$$\int_0^1 ds |\varphi_n(s)|^2 \approx h \sum_{\ell=0}^N [\varphi_n(s_\ell)]^2 \stackrel{!}{=} 1. \quad (10.56)$$

Consistently, we approximate the expectation value  $\langle s \rangle$  via

$$\int_0^1 ds s |\varphi_n(s)|^2 \approx h \sum_{\ell=0}^N [\varphi_n(s_\ell)]^2 s_\ell. \quad (10.57)$$

**Table 10.1** Comparison between analytic and numerical eigenenergies for the particle in a box for  $N = 100$

| $n$ | $\varepsilon_n$ -analytic | $\varepsilon_n$ -numeric |
|-----|---------------------------|--------------------------|
| 1   | 4.934802                  | 4.934802                 |
| 2   | 19.739209                 | 19.739208                |
| 3   | 44.413219                 | 44.413205                |
| 4   | 78.956835                 | 78.956753                |
| 5   | 123.370055                | 123.369742               |
| 6   | 177.652879                | 177.651943               |
| 7   | 241.805308                | 241.802947               |
| 8   | 315.827341                | 315.822077               |
| 9   | 399.718978                | 399.708300               |
| 10  | 493.480220                | 493.460113               |

The NUMEROV shooting algorithm is then defined by the following steps:

1. Choose two trial energies  $\varepsilon_a$  and  $\varepsilon_b$  and define the required accuracy  $\eta$ .
2. Calculate  $\varphi(s_N; \varepsilon_a) \equiv \varphi_a$  and  $\varphi(s_N; \varepsilon_b) \equiv \varphi_b$  using Eq. (10.54).
3. If  $\varphi_a \varphi_b > 0$ , choose new values for  $\varepsilon_a$  or  $\varepsilon_b$  and go to step 1.
4. If  $\varphi_a \varphi_b < 0$ , calculate  $\varepsilon_c = (\varepsilon_a + \varepsilon_b) / 2$  and determine  $\varphi(s_N; \varepsilon_c) \equiv \varphi_c$  using Eq. (10.54).
5. If  $\varphi_a \varphi_c < 0$ , set  $\varepsilon_b = \varepsilon_c$  and go to step 4.
6. If  $\varphi_c \varphi_b < 0$ , set  $\varepsilon_a = \varepsilon_c$  and go to step 4.
7. Terminate the loop when  $|\varepsilon_a - \varepsilon_b| < \eta$ .

These steps have been carried out for 100 grid-points, a potential  $\tilde{v} = 0$ , and a required accuracy of  $\eta = 10^{-10}$ . The first ten eigenenergies are given in Table 10.1 and are compared with analytic results (10.40).

In addition, Fig. 10.1 presents the first five eigenvalues  $\varepsilon_n$  (right hand scale) as horizontal straight lines. Aligned with these eigenvalues we find on the right hand side of this figure the corresponding normalized eigenfunctions calculated using  $N = 100$  grid-points. The agreement with the analytic result of Eq.(10.41) is excellent.

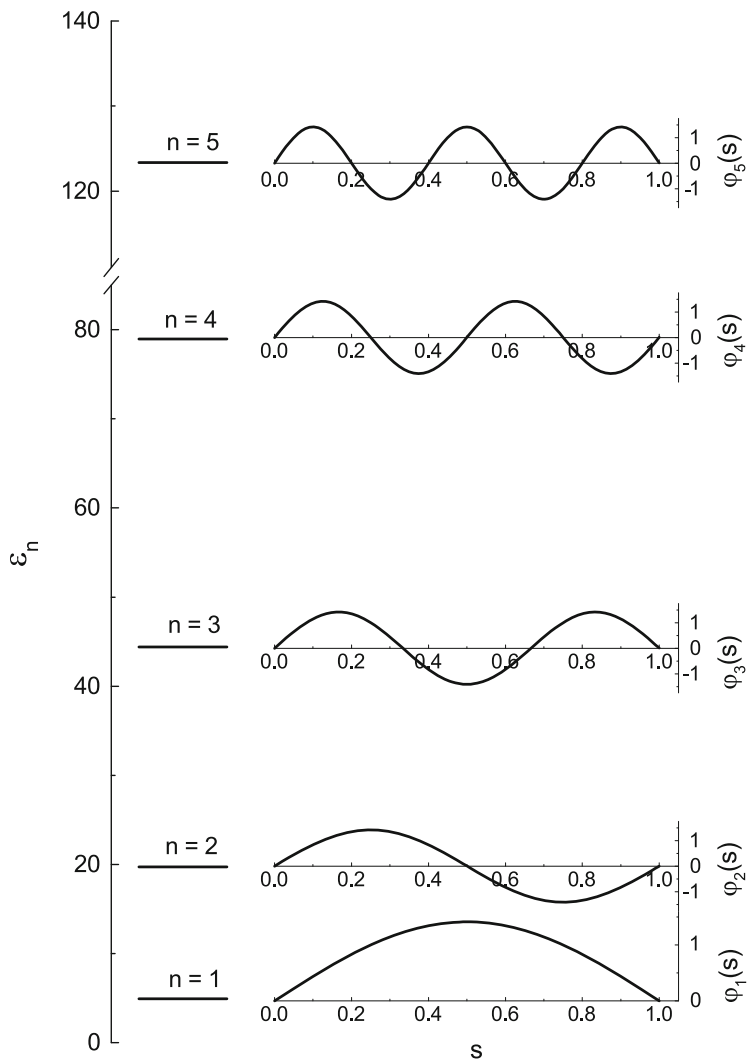


**Fig. 10.1** The first five numerically determined eigenvalues  $\varepsilon_n$  of Table 10.1 are presented as horizontal lines (left hand scale). Aligned with these eigenvalues are the corresponding eigenfunctions  $\varphi_n(s)$  vs  $s$  for  $N = 100$  (right hand scales)

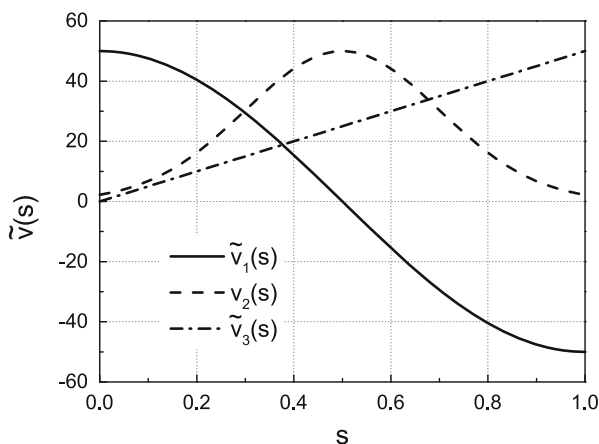
## 10.4 Another Case

Here we discuss briefly some results achieved with the help of NUMEROV's shooting algorithm. In particular, we discuss the particle in the box for three different potentials  $\tilde{v}(s)$

$$\tilde{v}_1(s) = 50 \cos(\pi s) , \quad \tilde{v}_2(s) = 50 \exp \left[ -\frac{(s - \frac{1}{2})^2}{0.08} \right] , \quad \tilde{v}_3(s) = 50s . \quad (10.58)$$

The potentials are illustrated in Fig. 10.2. All calculations were carried out with  $N = 100$  grid-points and an accuracy  $\eta = 10^{-10}$ . The first five eigenenergies  $\varepsilon_n$  are shown in Figs. 10.3, 10.4, and 10.5, respectively, as horizontal lines (left hand scale). The numerically determined normalized eigenfunctions  $\varphi_n(s)$  vs  $s$  (solid lines) are presented on the right hand side of these figures and are aligned with their respective eigenvalues. They are also compared with the eigenfunctions (dotted lines) of the particle in a box, i.e.  $\tilde{v}(s) = 0$ . In all cases the eigenfunctions reflect the symmetry of the various potentials  $\tilde{v}(s)$  which becomes particularly transparent in Fig. 10.3 for the potential  $\tilde{v}_1(s)$ . The eigenfunctions develop an additional node in comparison to the eigenfunctions calculated for  $\tilde{v}(s) = 0$ . In the other two cases only the very first eigenfunctions  $n \geq 3$  appear to be affected by the potential. Moreover, in all three cases, the respective eigenvalues are shifted towards higher values which is consistent with a general result of quantum mechanical perturbation theory.

**Fig. 10.2** The three different potentials  $\tilde{v}(s)$  defined in Eq. (10.58)



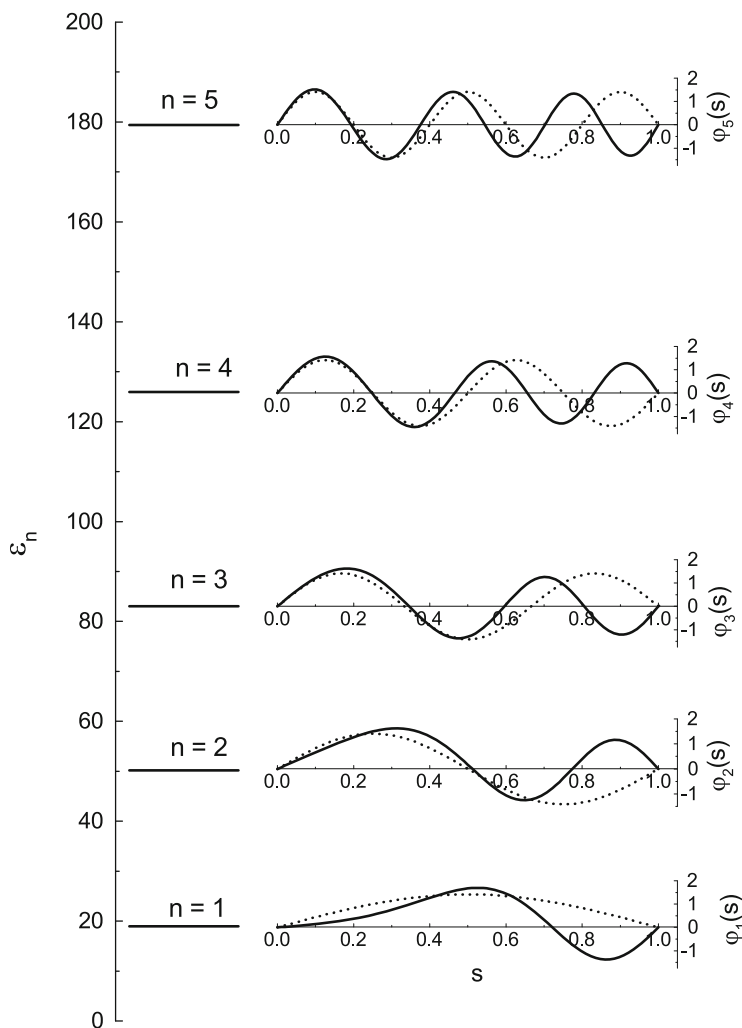


**Fig. 10.3** Numerically determined eigenvalues  $\varepsilon_n$  (left hand scale) and eigenfunctions  $\varphi_n(s)$  vs  $s$  (right hand scales) for the potential  $\tilde{v}_1(s)$ . The first five eigenvalues are presented as straight horizontal lines. Aligned with these lines the eigenfunctions are shown on the right hand side of this figure. The dotted lines indicate the eigenfunctions of the particle in the box with  $\tilde{v}(s) = 0$  (see Fig. 10.1)

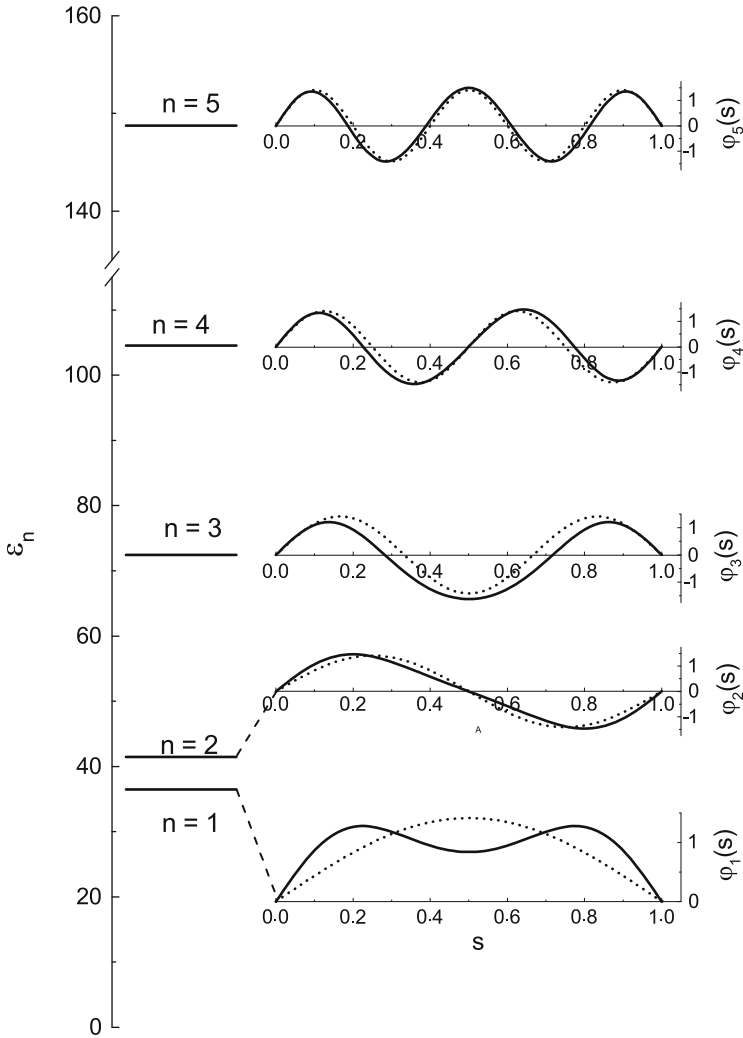


**Fig. 10.4** Numerically determined eigenvalues  $\epsilon_n$  (left hand scale) and eigenfunctions  $\phi_n(s)$  vs  $s$  (right hand scales) for the potential  $\tilde{v}_2(s)$ . The first five eigenvalues are presented as straight horizontal lines. Aligned with these lines the eigenfunctions are shown on the right hand side of this figure. The dotted lines indicate the eigenfunctions of the particle in the box with  $\tilde{v}(s) = 0$  (see Fig. 10.1)

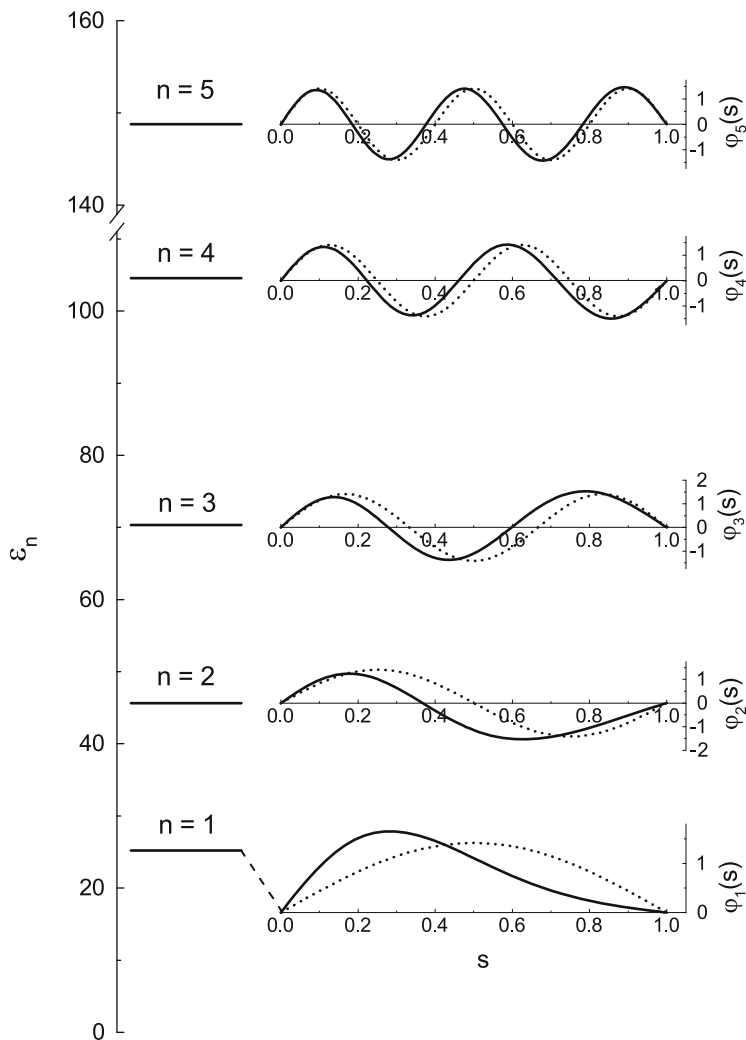


**Fig. 10.5** Numerically determined eigenvalues  $\varepsilon_n$  (left hand scale) and eigenfunctions  $\phi_n(s)$  vs  $s$  (right hand scales) for the potential  $\tilde{v}_3(s)$ . The first five eigenvalues are presented as straight horizontal lines. Aligned with these lines the eigenfunctions are shown on the right hand side of this figure. The dotted lines indicate the eigenfunctions of the particle in the box with  $\tilde{v}(s) = 0$  (see Fig. 10.1)

## Summary

The quantum-mechanical problem of a particle in a box was described by a homogeneous boundary value problem which could be solved analytically if the box' potential  $\tilde{v}(s) = 0$ . On the other hand, NUMEROV's shooting algorithm was particularly designed to treat effectively homogeneous boundary value problems. Consequently, the problem of the particle in the box was used to design a NUMEROV shooting algorithm which was then tested against the analytic results. The agreement between numerics and analytical results turned out to be excellent and proved the quality of the method. For illustrative purposes the problem of the particle in the box was then solved numerically for three different, more complex, box-potentials  $\tilde{v}(s)$ .

## Problems

1. Solve the one-dimensional stationary SCHRÖDINGER equation in an infinitely deep potential well by employing the shooting method according to NUMEROV of Sect. 8.3. The total potential  $v(s)$  is assumed to be of the form (10.51). Choose different potentials  $\tilde{v}(s)$  within the well.

You can check your code by reproducing the results presented in Sects. 10.3 and 10.4. In addition, determine numerically the expectation value  $\langle x \rangle$  and the variance  $\text{var}(x)$  of the position operator  $x$  for the first five eigenfunctions. This can be achieved by employing the rectangular rule of Chap. 3, as illustrated in Eq. (10.57).

2. Solve the SCHRÖDINGER equation for some potential  $\tilde{v}(s)$  of your choice and plot the first five eigenfunctions. This potential should not be equal to one of the potentials discussed in this chapter. Again, calculate  $\langle x \rangle$  and  $\text{var}(x)$  for the first five eigenfunctions.
3. Solve the stationary SCHRÖDINGER equation (10.4) for the harmonic potential  $V(x) = m\omega^2 x^2/2$ . The algorithm discussed in this chapter can be applied by choosing the box length  $L$  sufficiently large, so that the harmonic oscillator potential is well within the box for all energies of interest.
4. Solve the SCHRÖDINGER equation for a double well potential which can be obtained by adding two mutually displaced harmonic potentials.

## References

1. Baym, G.: Lectures on Quantum Mechanics. Lecture Notes and Supplements in Physics. The Benjamin/Cummings Publ. Comp., Inc., London/Amsterdam (1969)
2. Cohen-Tannoudji, C., Diu, B., Laloë, F.: Quantum Mechanics, vol. I. Wiley, New York (1977)
3. Sakurai, J.J.: Modern Quantum Mechanics. Addison-Wesley, Menlo Park (1985)

4. Ballentine, L.E.: Quantum Mechanics. World Scientific, Hackensack (1998)
5. Courant, R., Hilbert, D.: Methods of Mathematical Physics, vol. 1. Wiley, New York (1989)
6. Hairer, E., Nørsett, S.P., Wanner, G.: Solving Ordinary Differential Equations I. Springer Series in Computational Mathematics, vol. 8, 2nd edn. Springer, Berlin/Heidelberg (1993)